ChemComm

COMMUNICATION

View Article Online
View Journal | View Issue





Cite this: *Chem. Commun.*, 2022, **58**, 5789

Received 24th March 2022,
Accepted 14th April 2022

DOI: 10.1039/d2cc01696f

rsc.li/chemcomm

# Self-assembling figure-of-eight and pseudoplectoneme aromatic oligoamide ribbons†

Chenhao Yao,[a] Brice Kauffmann,[b] Ivan Huc *[cd] and Yann Ferrand *[a]

**Two oligoamide macrocycles composed of eight and twelve 7-amino-8-fluoro-2-quinolinecarboxylic acid monomers were synthesised despite the propensity of their acyclic precursors to fold and self-assemble into double helices. Macrocyclisations were made possible through the transient use of helicity disruptors. The resulting macrocyclic ribbons were found to adopt figure-of-eight and pseudoplectoneme shapes that maintain an ability to self-assemble.**

Macrocycles derived from frustrated foldamer helices‡ are molecules that would adopt a helical conformation upon ring-opening and whose inherent conformational preferences can't all be fulfilled in the cyclic form. The constraints that derive from conformational frustration often lead to molecular shapes not reachable by other means.[1] Besides, without conformational frustration, a helical foldamer would not macrocyclise as its two ends diverge from each other. The strain induced by the macrocyclisation decreases conformational freedom, gives access to unusual conformations and, more often than not, reveals peculiar properties and reactivities. Macrocycles derived from frustrated foldamer helices can thus in many ways be compared to other types of strained macrocycles including hydrocarbon belts,[2] infinitene,[3] cycloparaphenylenes,[4] macrocycles bearing angle-strained alkynes,[5] expanded porphyrinoids.[6] In this study, we report on the conformational frustration of aromatic oligoamide sequences that form stable double helices in solution. Previously, we demonstrated that the macrocyclisation of stable single helices of 8-amino-2-quinolinecarboxylic Q (2.5 units per turn), ranging from 5 to 7 units, was made possible by the transient use of local disruptor of helicity.[1b,c] Specifically, using acid labile dimethoxybenzyl (DMB) groups for the alkylation of secondary amide functions led to the destabilisation of the canonical folding of aromatic oligoamide helices and allowed for their macrocyclisation.

Besides single helices, some aromatic oligoamide sequences have a strong propensity to self-assemble into double helical dimers. This applies in particular to monomers coding for a wide diameter because of the lower energy cost of spring-like extension associated with double helix formation (Fig. 1(a), top right).[7] In the case of oligoamides of 7-amino-8-fluoro-2-quinolinecarboxylic acid ($Q^F$), the predicted curvature is *ca.* 4 units per turn. $Q^F_8$, an oligomer that spans about two turns, revealed a high dimerisation constant ($K_{dim}$) of almost $10^6$ L mol$^{-1}$ in chloroform. Elongating a sequence beyond eight units[7b] is low yielding because of the steric hindrance at the strand termini associated with folding and double helix formation. Notwithstanding elongation, the direct cyclisation of long fluoroquinoline oligoamides is simply impossible. We devised that the alkylation with DMB groups of few secondary amide functions of $Q^F$ oligomers might perturb simultaneously the folding of the helical strands as well as their propensity to self-assemble so as to allow macrocyclisation (Fig. 1(a), top left). Indeed, the use of DMB groups has been validated before to prevent aggregation of aromatic oligoamides rods[8] and to decrease hindrance in single helices.[9]

Octameric and dodecameric macrocycles **1b** and **2b** (Fig. 1(b)) were synthesised following a convergent strategy as described in detail in the ESI.† We assumed that one DMB tertiary amide bond per helix turn would be sufficient to prevent correct folding. Thus, an octamer would be alkylated twice whereas a dodecamer would contain three DMB groups. The DMB-containing cyclo-octamer **1a** and cyclo-dodecamer **2a** were obtained from their respective acyclic amino acid precursors using *in situ* acid chloride activation with $Cl_3CCN/PPh_3$ (Fig. S3 and S4, ESI†).[1b,c] A two-step purification of the cyclic products was required using first silica gel chromatography to

[a] *Univ. Bordeaux, CNRS, Bordeaux Institut National Polytechnique, CBMN UMR 5248, 2 rue Escarpit, 33600 Pessac, France. E-mail: yann.ferrand@u-bordeaux.fr*
[b] *Univ. Bordeaux, CNRS, INSERM, Institut Européen de Chimie Biologie (UMS3033/US001), 2 rue Escarpit, 33600 Pessac, France*
[c] *Department Pharmazie, Ludwig-Maximilians-Universität, Butenandtstr. 5–13, 81377 München, Germany*
[d] *Cluster of Excellence e-conversion, 85748 Garching, Germany. E-mail: ivan.huc@cup.lmu.de*

† Electronic supplementary information (ESI) available: Single crystals suitable for X-ray diffraction analysis were obtained by slow liquid–liquid diffusion. CCDC 2160708 (**1b**) and 2161479 (**2b**)$_2$. For ESI and crystallographic data in CIF or other electronic format see DOI: https://doi.org/10.1039/d2cc01696f

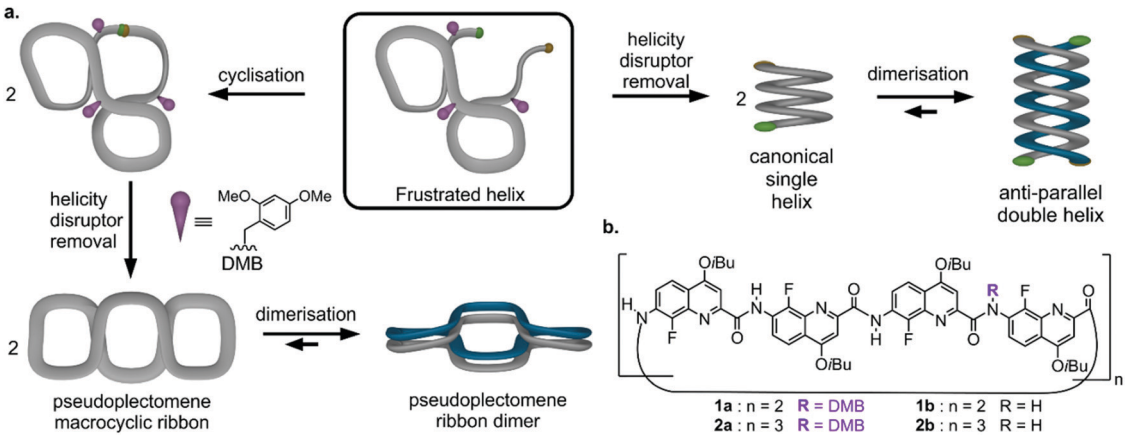


Fig. 1 (a) Schematic representation of the strategy used to macrocyclise a strand that tends to fold and to self-assemble in a double helix; (top right) single helix–double helix equilibrium. (Top left) introduction of a helicity disruptor on an aromatic strand preventing it from folding and from dimerising. The helicity disruptors (DMB groups, purple) allow for the cyclisation of the strand and a constrained macrocycle is obtained after their removal. (Bottom left) to satisfy the propensity of the strand to form helices, the strand can adopt a ribbon shape that can be twisted multiple times. A second property inherited from its original double helical nature is that the strand can form a pseudo plectonemic arrangement upon dimerizing. (b) Formulae of the macrocycles and their DMB-protected precursors.

remove the unreacted amino acid precursor and other polar non-cyclic polymers, and then recycling GPC (Fig. S9 and S10, ESI†) to obtain **1a** or **2a** in 36% and 61% yield, respectively. Secondary amides were recovered using TFA-mediated cleavage of the DMB groups at 60 °C to yield macrocycles **1b** and **2b** quantitatively.

The identity of the cyclo-octamer was first confirmed by electrospray mass spectrometry (ESI-MS). Surprisingly **1b** was only detected at $m/z$ = 2082.5 as a trication, and 1562.4 as a tetracation which correspond to a $(\mathbf{1b})_3$ trimeric species (Fig. S11, ESI†). We then tried to decipher the folding conformation of **1b** in solution using NMR. In most solvents the $^1$H and $^{19}$F NMR spectra of **1b** at room temperature revealed broad lines indicating most probably some sort of aggregation (Fig. S1 and S2, ESI†) in accordance with the results of mass spectrometry. The $^1$H NMR spectrum in $C_2D_2Cl_4$ showed sharper resonances but it remained too complex for a detailed structural investigation. Upon increasing the temperature to 353 K coalescence was almost reached hinting at the coexistence of multiple aggregated species in exchange (Fig. S3, ESI†).

The structure of macrocycle **1b** was elucidated in the solid state by X-ray crystallography.† It revealed a figure-of-eight shape combining two helical segments, each spanning one turn including four $Q^F$ monomers. As observed for $Q_n$ macrocycles[1b,c] the two rings are connected by two local disruptions of the preferred conformation (Fig. 2(c) *vs.* Fig. 2(d)). Both consist of a 180° flip of a $Q^F$ unit about the fluorobenzene – nitrogen amide bond, forcing the fluorine atom in position 8 to face the carbonyl of the adjacent quinoline ring despite the electronic repulsion between their lone pairs. An outcome of the repulsion is that the two consecutive $Q^F$ are not in the same plane anymore (Fig. 2(d)–(f)). Extensive macrocycle-macrocycle contacts are observed in the crystal lattice that are perhaps related to aggregation observed in solution phase. First, two macrocycles of similar handedness intertwine *via* the intercalation of one their loops (Fig. 2(b)) forming a triangular

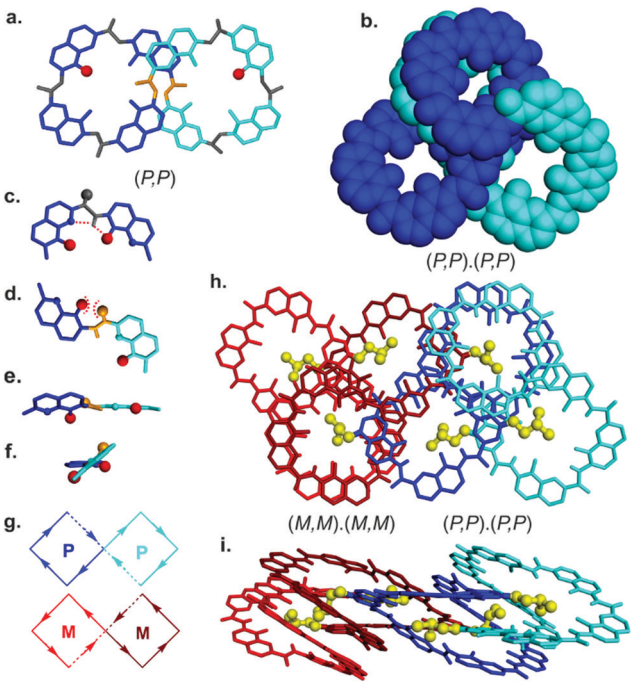


Fig. 2 X-ray structure of **1b**: (a) top view of the eight-shape macrocycle, the two *P* helical segments are shown in blue and light blue tube representation. The amide bonds in grey tube adopt the preferred conformation whereas the ones highlighted in yellow are flipped; two fluorine atoms (out of 8) are shown as red balls. (b) Top view of a triangle-shape *P,P*-$(\mathbf{1b})_2$ dimer shown in space filling representation; (c) preferred folding mode of the amide bond *vs.* (d) Flipped mode. (e) front and (f) side view of the flipped mode. (g) Schematic representation of the folding of **1b** where the two cycles adopt the same handedness, either *P* (blue) or *M* (red). Each straight line represents a $Q^F$ unit. In the crystal lattice, the macrocycle exists as *M,M* or *P,P* enantiomers; the space group *P*21/*c* is centrosymmetrical. (h) Top and (i) side view of the tetrameric assembly $(\mathbf{1b})_4$ consisting of the interdigitation of two (*P,P*).(*P,P*) and (*M,M*).(*M,M*) triangle shaped $(\mathbf{1b})_2$, shown in blue and red, respectively. Included solvent molecules have been removed for clarity. Helix side chains (OiBu groups) have also been removed except in (h and i) where they can be seen to penetrate the closest helical cavity (yellow balls and sticks).

 

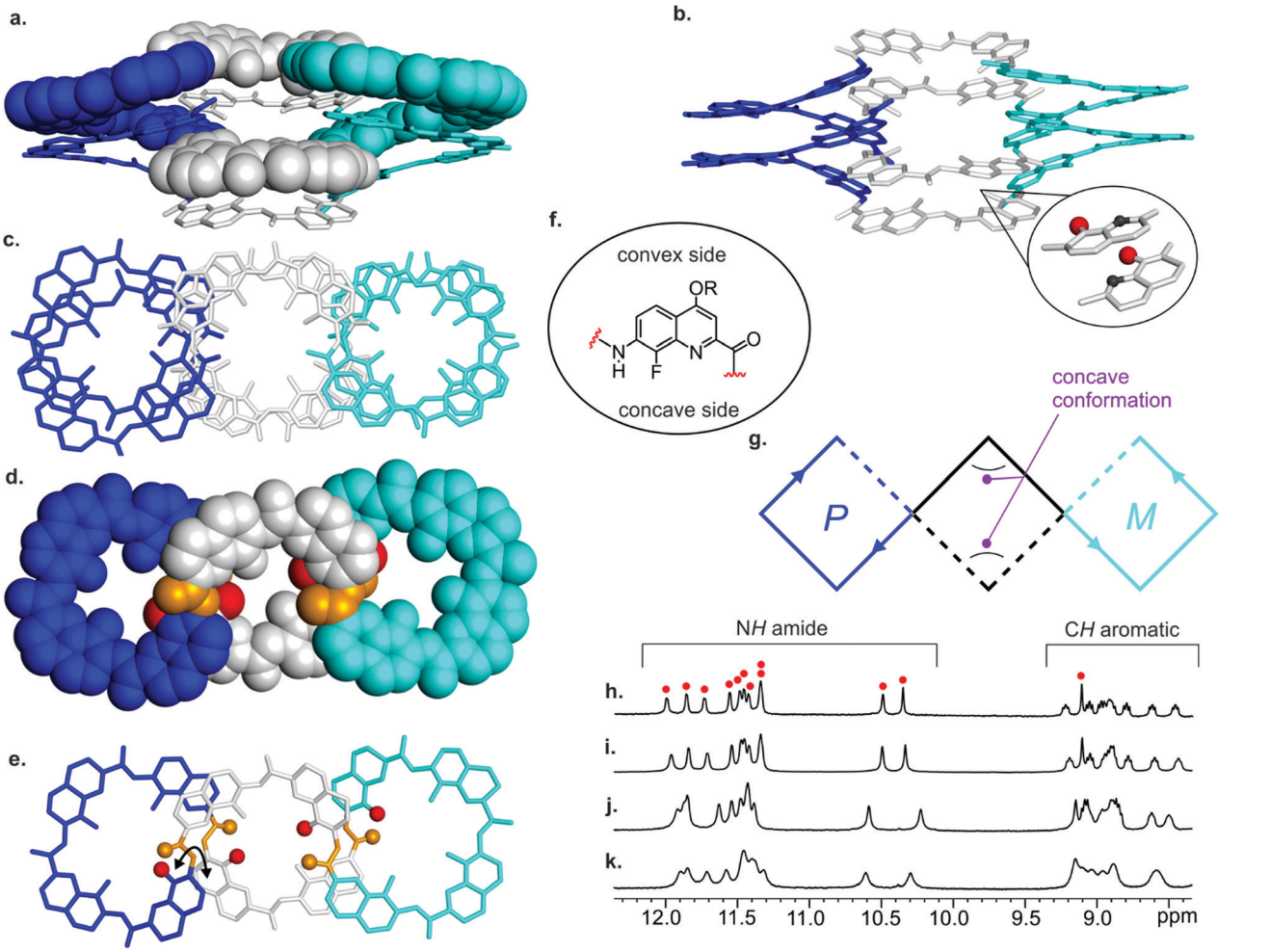


Fig. 3 X-ray structure of $(\mathbf{2b})_2$: (a) front view showing one strand in space filling representation whereas the second one is shown in tube representation; (b) front view in tube representation and zoom of two $Q^F$ monomers in antiparallel arrangement; (c) top view in tube representation. (d) and (e) top view of a single strand of $(\mathbf{2b})_2$ shown in space filling and tube representation, respectively. The black double-headed arrow in (e) denotes the rotation about the fluorobenzene/nitrogen amide bond. In (a)–(e) the *P* and *M* helical segments are show in blue and light blue, respectively, whereas the central flipped $Q^F{}_2$ segments are shown in white. Some fluorine atoms are shown as red balls whereas flipped carbonyl are represented as golden balls. Isobutoxy side chains (OiBu) and included solvent molecules have been removed for clarity. (f) Definition of the convex and concave side of a $Q^F$ unit. (g) Schematic representation of **2b** highlighting the *P*,*M* helicity and the concave conformations. Part of the 400 MHz $^1$H NMR spectra of **2b** at: (h) 0.1 mM, 298 K, in $CDCl_3$; (i) 3.2 mM, 298 K, in $CDCl_3$; (j) 0.5 mM, 298 K, in $C_2D_2Cl_4$; (k) 0.5 mM, 353 K, in $C_2D_2Cl_4$. The red circles denote the 12 amide protons.

shape dimer $(\mathbf{1b})_2$. Then, two enantiomeric triangular dimers $(\mathbf{1b})_2$ that is (*P*,*P*).(*P*,*P*) and (*M*,*M*).(*M*,*M*) can interdigitate to form a well-defined quaternary assembly $(\mathbf{1b})_4$ of imbricated figure-of-eight macrocycles (Fig. 2(f)). The interdigitation seems to be directly inherited from the propensity of the noncyclic sequences to form double helices and is associated to the low energy cost of increasing the helix pitch of $Q^F$ oligomers (see above). Additionally, penetration of some isobutoxy side chains into neighbouring helix cavities further enhance intermolecular contacts (Fig. 2(h) and (i), yellow).

Single crystals of **2b** were also obtained from the diffusion of hexane in a chloroform solution of the dodecameric macrocycle and its solid state structure was solved in the $P\bar{1}$ space group. The crystalline structure revealed an unprecedented $(\mathbf{2b})_2$ architecture composed of two intercalated aromatic ribbons (Fig. 3(a)–(c)). Each dodecameric cyclic strand displayed four twisted $Q^F$ units coloured in white in Fig. 3. By analogy with the convention established for porphyrinoids,[10] macrocycle **2b** possesses a quadriconcave conformation (Fig. 3(d)–(g)). Each concave conformation occurs at a $Q^F$ unit that is flipped with respect to the naturally convex curvature of the macrocycle (see ref. 10 for a detailed presentation). A pair of flipped units generates a crossing so the structure has two crossings (Fig. 3(d) and (e)). One can note that, as for **1b** and contrarily to some Q macrocycles,[1b,c] no *cis* amide conformation is involved. Instead, $Q^F$ units rotate about 180° about the bond linking their fluorobenzene ring and the neighbouring amide NH (Fig. 3(e), black double-headed arrow). Overall, the resulting macrocycle structure has two full helical turns (*i.e.* each comprised of four $Q^F$ units) with opposite *P* and *M* handedness connected by two concave bridges, one above and one below the median plane of the macrocycle (Fig. 3(d), (e) and (g)).

Swapping the above/below position of the two bridges would lead to the inversion of both helices. Like some *meso* helices,[11] this macrocycle possesses a centre of symmetry. As the macrocycle contains an even number (2) of crossings the macrocyclic architecture can be termed pseudoplectoneme by analogy with plectonemic conformations of DNA.[10] It should be emphasized that the ribbon is not twisted in contrary to the figure-of-eight shape of **1b**.

The propensity of $Q^F$ oligomers to self-assemble is expressed in the structure of **2b** under the form of discrete dimers. A doubling of helix pitch is required to form a double helix from two single helices in acyclic oligomers. The same extension of a cyclic ribbon enables the intercalation of a second strand without alteration of the overall shape (Fig. 1(a), bottom left). The dimer shows extensive intermolecular aromatic stacking. Electrostatics probably drive the opposite N-to-C orientation of the two cyclic ribbons within the dimer (Fig. 3(b), zoom). Within the dimeric assembly, the two macrocycles are equivalent. However, the assembly results in a loss of symmetry: within each macrocycle, all twelve $Q^F$ units are distinct. Such loss of symmetry has been reported in other large homomeric macrocycles.[12] Furthermore, contrary to the individual achiral $C_i$ symmetrical monomers, the dimeric assembly is chiral with an overall axial $C_2$ symmetry (Fig. S16, ESI†). Chirality can be reverted by taking the macrocycle ''below'' within the stack, and translating it ''above'' without any rotation.

The structure and aggregation properties of **2b** in solution were probed by NMR. The $^1$H NMR of the dodecameric macrocycle in $CDCl_3$ revealed a single set of 12 sharp amide resonances (Fig. 3(f)), a number that is twice as large as the theoretical six resonances than can be expected for the $C_i$ symmetry of the single stranded **2b** but that corresponds exactly to $C_2$-symmetrical dimer $(\mathbf{2b})_2$. The twelve fluorine resonances detected by $^{19}$F NMR also confirmed that the dimer form is the prevalent species in solution. Diluting a solution of $(\mathbf{2b})_2$ in $CDCl_3$ or tetrachloroethane-$d_2$ did not reveal any traceable amount of single stranded macrocycle. No significant changes can be observed neither upon heating the same sample at 353 K (Fig. 3(i)). These experiments gave a minimal estimate of the dimerization constants ($K_{dim}$) of $10^8$ L mol$^{-1}$. They also indicate that fluxionality within the macrocycle is slow on the NMR timescale at this temperature.

We have shown that macrocyclisation of $Q^F$ oligomers leads to new expressions of their propensity to fold into helices and to assemble into double-stranded dimers. One may speculate that other cyclo-$Q^F_{4n}$ oligomers may form shapes similar to those of cyclo-$Q^F_8$ and cyclo-$Q^F_{16}$ by combining twisted and pseudoplectoneme motifs. The self-assembly of macrocycles by strand intercalation is novel and contrasts with the more classical stacking of flat shape-persistent rings.[13–16]

This work was supported by the China Scholarship Council (pre-doctoral fellowship to C. Y.). We thank the France-Germany International Research Project ''Foldamers Structures and Functions'' (IRP FoldSFun). This work has benefited from the facilities and expertise of the Biophysical and Structural Chemistry platform (BPCS) at IECB, CNRS UAR3033, Inserm US001, and Bordeaux University.

## Conflicts of interest

There are no conflicts to declare.

## Notes and references

‡ Frustrated foldamer helices can be defined as foldamers whose helical folding propensity is frustrated, *e.g.* by macrocyclization, preventing the fulfillment of some conformational preferences.

1 (*a*) Z. Zhang, W.-Y. Cha, N. J. Williams, E. L. Rush, M. Ishida, V. M. Lynch, D. Kim and J. L. Sessler, *J. Am. Chem. Soc.*, 2014, **136**, 7591; (*b*) K. Urushibara, Y. Ferrand, Z. Liu, H. Masu, V. Pophristic, A. Tanatani and I. Huc, *Angew. Chem., Int. Ed.*, 2018, **57**, 7888; (*c*) K. Urushibara, Y. Ferrand, Z. Liu, K. Katagiri, M. Kawahata, E. Morvan, R. D'Elia, V. Pophristic, A. Tanatani and I. Huc, *Chem. – Eur. J.*, 2021, **27**, 11205.
2 (*a*) G. Povie, Y. Segawa, T. Nishihara, Y. Miyauchi and K. Itami, *Science*, 2017, **356**, 172; (*b*) Y. Segawa, M. Kuwayama, Y. Hijikata, M. Fushimi, T. Nishihara, J. Pirillo, J. Shirasaki, N. Kubota and K. Itami, *Science*, 2019, **365**, 272; (*c*) T.-H. Shi, Q.-H. Guo, S. Tong and M.-X. Wang, *J. Am. Chem. Soc.*, 2020, **142**, 4576.
3 M. Krzeszewski, H. Ito and K. Itami, *J. Am. Chem. Soc.*, 2022, **144**, 862.
4 (*a*) S. Yamago, Y. Watanabe and T. Iwamoto, *Angew. Chem., Int. Ed.*, 2010, **49**, 757; (*b*) S. Mirzaei, E. Castro and R. Hernandez Sanchez, *Chem. Sci.*, 2020, **11**, 8089; (*c*) N. K. Mitra, C. P. Merryman and B. L. Merner, *Synlett*, 2017, 2205.
5 K. Miki and K. Ohe, *Chem. – Eur. J.*, 2020, **26**, 2529.
6 (*a*) J.-Y. Shin, H. Furuta, K. Yoza, S. Igarashi and A. Osuka, *J. Am. Chem. Soc.*, 2001, **123**, 7190; (*b*) J.-i. Setsune and S. Maeda, *J. Am. Chem. Soc.*, 2000, **122**, 12405; (*c*) L. Latos-Grazynski, *Angew. Chem., Int. Ed.*, 2004, **43**, 5124; (*d*) S. Shimizu, W.-S. Cho, J. L. Sessler, H. Shinokubo and A. Osuka, *Chem. – Eur. J.*, 2008, **14**, 2668.
7 (*a*) E. Berni, B. Kauffmann, C. Bao, J. Lefeuvre, D. M. Bassani and I. Huc, *Chem. – Eur. J.*, 2007, **13**, 8463; (*b*) Q. Gan, C. Bao, B. Kauffmann, A. Grélard, J. Xiang, S. Liu, I. Huc and H. Jiang, *Angew. Chem., Int. Ed.*, 2008, **47**, 1715.
8 H. M. König, R. Abbel, D. Schollmeyer and A. F. M. Kilbinger, *Org. Lett.*, 2006, **8**, 1819.
9 A. Zhang, J. S. Ferguson, K. Yamato, C. Zheng and B. Gong, *Org. Lett.*, 2006, **8**, 5117.
10 M. Stepien, N. Sprutta and L. Latos-Grazynski, *Angew. Chem., Int. Ed.*, 2011, **50**, 4288.
11 V. Maurizot, C. Dolain, Y. Leydet, J.-M. Léger, P. Guionneau and I. Huc, *J. Am. Chem. Soc.*, 2004, **126**, 10049.
12 C. G. Pappas, P. K. Mandal, B. Liu, B. Kauffmann, X. Miao, D. Komáromy, W. Hoffmann, C. Manz, R. Chang, K. Liu, K. Pagel, I. Huc and S. Otto, *Nat. Chem.*, 2020, **12**, 1180.
13 D. Zhao and J. S. Moore, *Chem. Commun.*, 2003, 807.
14 L. Shu and M. Mayor, *Chem. Commun.*, 2006, 4134.
15 X. Wu, R. Liu, B. Sathyamoorthy, K. Yamato, G. Liang, L. Shen, S. Ma, D. K. Sukumaran, T. Szyperski, W. Fang, L. He, X. Chen and B. Gong, *J. Am. Chem. Soc.*, 2015, **137**, 5879.
16 Y. Liu, J. Shen, C. Sun, C. Ren and H. Zeng, *J. Am. Chem. Soc.*, 2015, **137**, 12055.

 